Atomic data for modelling of photo-pumped lasers

K. McKeown, K. M. Aggarwal and F. P. Keenan
Department of Physics and Astronomy, The Queen's University of Belfast, Belfast, BT7 1NN, UK

P. H. Norrington
Department of Applied Mathematics and Theoretical Physics, The Queen's University of Belfast, Belfast, BT7 1NN, UK

S. J. Rose
Department of Physics, Clarendon Laboratory, Parks Road, Oxford, OX1 3PU, UK

Main contact email address k.mckeown@qub.ac.uk

Introduction

Line coincidence photo-pumping has been long accepted as a method by which X-ray lasing can be generated. In order to be able to effectively model potential lasing schemes, it is essential to have available reliable atomic data, such as energy levels, radiative rates, A_{ji} (in s^{-1}), and effective collision strengths, À (dimensionless).

Lee *et al.*,[1], and Al' Miev *et al.*,[2], have both investigated a photo-pumping scheme involving hydrogen-like aluminium, Al XIII, and lithium-like iron, Fe XXIV. The scheme detailed in[1] considered Ly-α2 ($2p_{1/2}$-$1s_{1/2}$) radiation from Al XIII pumping the ground-state of Fe XXIV up to 5*p* levels, while[2] also takes into consideration Ly-α_1 ($2p_{3/2}$-$1s_{1/2}$) radiation. The pumping part of the proposed scheme leads to collisional mixing between the other n = 5 levels, and it is from the population of these sub-levels that an inversion will occur and so lead to lasing. Gains are expected from transitions 5*g* - 4*f*, 5*f* - 4*d*, 5*d* - 4*p*, 5*p* - 4*s*.

Calculations for the ions detailed in[1] and[2] have been performed to determine atomic data to be used in further investigation and development of the lasing scheme. A full set of results; 25 fine-structure energy levels, A_{ji} and Y, for Al XIII have been published[3]. The results of the atomic structure calculation, 24 fine-structure levels, A_{ji} and oscillator strengths, of Fe XXIV are available in[4]. The collisional calculations for Fe XXIV are nearing completion.

In this brief report, results for Fe XXIV will be the focus. Illustrative results will be presented, including transitions involved in the photo-pumping scheme.

Calculations

For both Al XIII and Fe XXIV, the fine-structure energy levels (in both cases for $n \leq 5$) and A_{ji} were calculated using the General purpose Relativistic Atomic Structure Package (GRASP)[5]. This is a fully relativistic code based on *jj*-coupling, and subsequent comparison of our results, viz.[3],[4], shows the excellent agreement we attained, both in magnitude and ordering, with existing experimental and, in the case of Fe XXIV, theoretical results.

Calculations of collision strengths, Ω (dimensionless), were performed using the relativistic Dirac Atomic R-matrix Code (DARC)[6]. DARC incorporates relativistic effects in a systematic manner in both the target and channel description. It is based on *jj*-coupling and uses a Dirac-Coulomb Hamiltonian in an R-matrix approach. Details of the DARC calculation and the full results for Al XIII are given in[3].

For Fe XXIV, the R-matrix radius was taken as 4 atomic units, 80 continuum orbitals were retained for expanding the wave function for each channel angular momentum, and 108 was the maximum number of channels available for each partial wave, which corresponded to a maximum Hamiltonian size of 8640. Contributions from all partial waves with $J \leq 60$ have been included. The highest energy that Ω has been calculated up to is 1,000 Ryd, which allows Y to be computed to temperatures of over 10^7 K.

Results

There are two distinct regions in which our calculations have been performed: below highest threshold and above highest threshold. In both of these regions, we have calculated total Ω using a partial waves approach, and then determined Y, which are symmetric and defined as:

$$\Upsilon_{if}(T_e) = \int_0^\infty \Omega_{if}(E_f) e^{-E_f/kT_e} d(E_f/kT_e)$$

E_f is the kinetic energy of the continuum electron, T_e is the electron temperature in K, and k is Boltzmann's constant. The excitation rate, q_{ij}, and de-excitation rate, q_{fi}, are both simply related to Y as:

$$q_{if} = \frac{8.63\times10^{-6}}{\omega_i T_e^{1/2}} \Upsilon_{if}(T_e) e^{-\Delta E/kT_e} \quad \mathrm{cm^3 s^{-1}}$$

and

$$q_{fi} = \frac{8.63\times10^{-6}}{\omega_f T_e^{1/2}} \Upsilon_{if}(T_e) \quad \mathrm{cm^3 s^{-1}}$$

where ω_i and ω_f are the statistical weights of the lower and upper levels, respectively, and $\Delta E = E_f - E_i$.

Above Threshold

In this region, no resonances are present, and typically Ω is slowly convergent with increasing energy for electric dipole transitions, the so-called 'allowed transitions'.

Figure 1 considers three specific electric-dipole transitions: $1s^2 5d\ ^2D_{3/2} - 1s^2 4p\ ^2P^o_{1/2}$, $1s^2 5f\ ^2F^o_{5/2} - 1s^2 4d\ ^2D_{3/2}$, $1s^2 5g\ ^2G_{7/2} - 1s^2 4f\ ^2F^o_{5/2}$, at two energies -130 Ryd. and 250 Ryd., both of which lie above the highest threshold. The convergence of ø is clearly slower for the higher energy as the partial waves with higher J values contribute more to the total value of Ω. Since it is not computationally feasible to perform the DARC calculations beyond $J > 60$, we are able to account for the contribution of the higher neglected partial waves by utilizing a sum rule detailed in[7]. Using the Flexible Atomic Code (FAC)[8], a separate

calculation has been performed to permit comparison between values of Ω. An example of the agreement between the two calculations is shown in Figure 2.

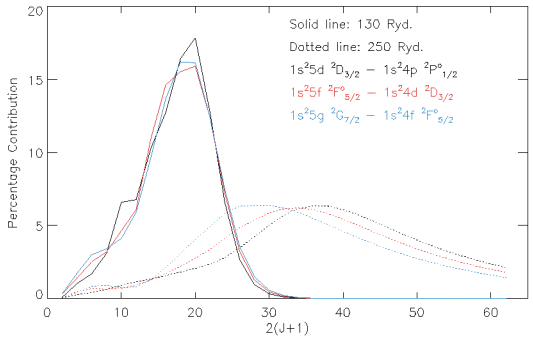

Figure 1. The percentage contribution to Ω for three allowed transitions expected to produce lasing.

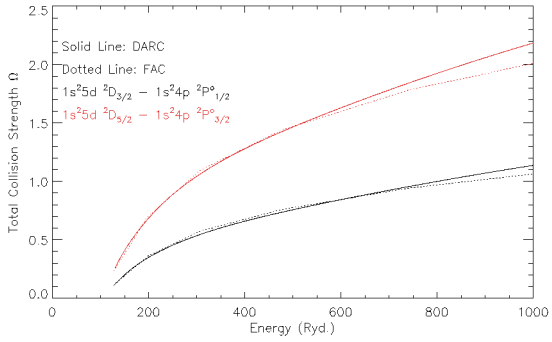

Figure 2. Ω calculated by DARC and FAC codes for two predicted lasing transitions.

Below Threshold

In the region lying below the highest threshold, resonances are prominent and their contribution must be accounted for. The resonances are delineated by performing the calculations on a fine energy mesh. Approaching a threshold, the mesh size was 0.0005 Ryd and this gradually increased to a maximum value of 0.002 Ryd moving between thresholds.

In the proposed lasing schemes, the transitions $1s^22s\ ^2S_{1/2} – 1s^25p\ 2P^o_{1/2}$ and $1s^22s\ ^2S_{1/2} – 1s^25p\ ^2P^o_{3/2}$ are the 'pumping' transitions. Figure 3 shows the occurrence of resonances in the threshold energy region. Despite the differences in magnitude of ø, the resonance pattern between the two transitions is very similar.

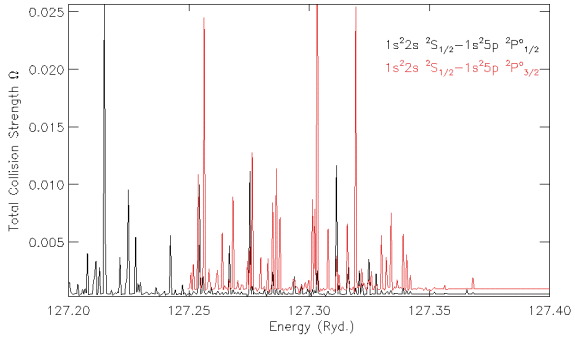

Figure 3. Resonance structure for 'pumping' transitions.

Rate Coefficients

Currently the calculations of Y, q_{if} and q_{if} are nearing completion, and a full set of results will soon be presented.

The lasing schemes consider both the $1s^25p\ ^2P^o_{1/2}$ and $1s^25p\ ^2P^o_{3/2}$ levels of Fe XXIV being pumped by Al XIII. In Figure 4 we plot the excitation rates for the pumping transitions $1s^22s\ ^2S_{1/2} – 1s^25p\ ^2P^o_{1/2}$ and $1s^22s\ ^2S_{1/2} – 1s^25p\ ^2P^o_{3/2}$.

Comparison of results will be made with those already available in the literature, and a full discussion will be reported with the full set of results. Here we will discuss briefly comparison with results of Berrington and Tully[9]. Their approach used a 2 step Breit-Pauli R-matrix technique, see[9] for further detail, which involved a target constructed from 15 fine-structure levels ($n \leq 4$). Figure 9 in their paper shows Y across the temperature range $4 \leq \log T_e(\mathrm{K}) \leq 8$, and clearly highlights the importance of resonances. A comparison is made with the distorted wave calculation of Zhang *et al.*,[10], and a 50% increase against the background is shown. In Figure 5 we show a comparison of our results across the region $6.2 \leq \log T_e(\mathrm{K}) \leq 8$, where the largest increase is observed. This clearly reinforces the importance for the inclusion and delineation of resonances.

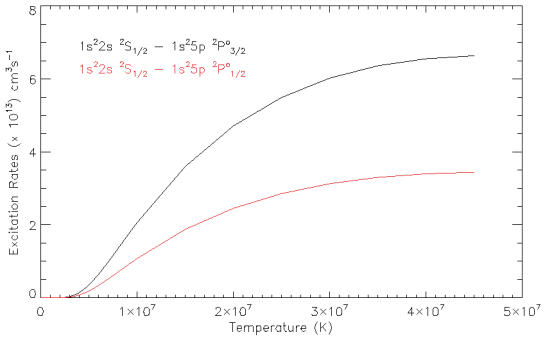

Figure 4. Excitation rate coefficients (×10[13]) for 'pumping' transitions.

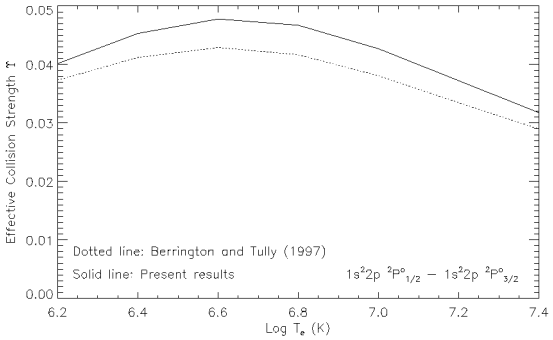

Figure 5. 'Comparison of Y values for forbidden transition $1s^22p_{1/2}\ ^2P^o_{1/2} – 1s^22p_{3/2}\ ^2P^o_{3/2}$.

Comparing results for the two transitions $1s^22s\ ^2S_{1/2} – 1s^24f\ ^2F^o_{5/2}$ and $1s^22s\ ^2S_{1/2} – 1s^24f\ ^2F^o_{7/2}$ in Figure 6, we can clearly see in the lower end of the temperature range disagreement of over 20%. Gradually as the temperature increases, agreement between the two sets of results improves. Inclusion of resonances is the likely explanation of the differences we observe between the two data sets. After detecting a finite number of resonances,

the search for resonances by Berrington and Tully would be ceased. This approach was not adopted is in our method, and it is likely that throughout our calculation we have pinpointed a higher number of resonances, which would then account for our higher values.

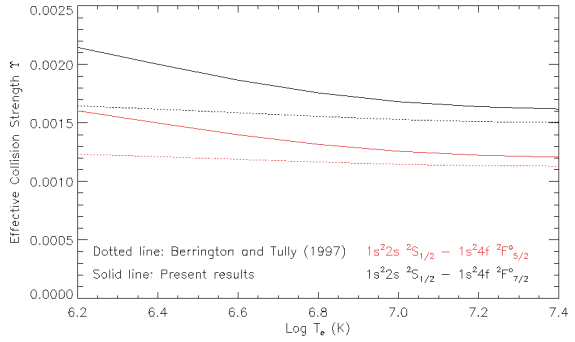

Figure 6. Comparison of Υ for forbidden transitions across the temperature range $6.2 \leq \log T_e(\mathrm{K}) \leq 7.4$.

Conclusions

In conclusion, for Al XIII we have calculated energy levels and radiative rates among the 25 fine-structure levels and for Fe XXIV energy levels and radiative rates among the 24 fine-structure levels. The energy levels calculated for both ions show excellent agreement in both magnitude and ordering with data already available in the literature. The radiative rates of Al XIII and Fe XXIV (with the exception of one transition) have been assessed to be accurate to 5%, which is highly satisfactory. The completed calculations, see[3] for more detail, of Al XIII highlighted the importance of the inclusion of relativistic effects due to the additional resonances observed when fine-structure was included in the definition of channel coupling, which leads to an increase in Υ.

Similar results for transitions in Fe XXIV will soon be reported, along with detailed comparisons with results already available in the literature.

Acknowledgements

The work reported in this report has been financed by ESPRC and PPARC of the United Kingdom. FPK and SJR are grateful to AWE Aldermaston for the award of William Penney Fellowships © British Crown Copyright 2004/MOD. KM acknowledges financial support from the Department of Education and Learning for Northern Ireland, and AWE Aldermaston.

References

1. Y. T. Lee, W.M. Howard and J.K. Nash, *J. Quant. Spect. Radiat. Transfer* **43** (1990) 335-345
2. I. R. Al'Miev, S. J. Rose and J. S. Wark, *J. Quant. Spect. Radiat. Transfer* **71** (2001) 129-138
3. K. M. Aggarwal, F. P. Keenan and S. J. Rose, *Astron. & Astrophys.* **432** (2005) 1151-1155
4. K. McKeown, K. M. Aggarwal, F. P. Keenan and S. J. Rose, *Phys. Scr.* **70** (2004) 295-303
5. K. G. Dyall, I. P. Grant, C. T. Johnson, F. A. Parpia and E. P. Plummer, *Comput. Phys. Commun.* **55** (1989) 424-456
6. S. Ait-Tahar, I. P. Grant and P. H. Norrington, *Phys. Rev. A* **54** (1996) 3984-3989. www.am.qub.ac.uk/DARC
7. V. M. Burke and M. J. Seaton, *J. Phys. B: At. Mol. Phys.* **19** (1986) L527-L533
8. M. F. Gu, *ApJ* **582** (2003) 1241-1250
9. K. A. Berrington and J. A. Tully, *Astron. & Astrophys. Suppl. Ser.* **126** (1997) 105-111
10. H. L. Zhang, D. H. Sampson, C. J. Fontes, *Atom. Data Nucl. Data Tab.* **44** (1990) 31-77